Title	Characteristics of supercontinuum generation under the influence of a weak continuous-wave trigger
Author(s)	Li, Q; Li, F; Wong, KKY; Lau, APT; Tsia, KK; Wai, PKA
Citation	The 24th Annual Meeting of the IEEE Photonics Society (PHO 2011), Arlington, VA., 9-13 October 2011. In Proceedings of 24th IEEE PHO, 2011, p. 53-54
Issued Date	2011
URL	http://hdl.handle.net/10722/140234
Rights	Proceedings of the IEEE Photonics Society (PHO). Copyright © IEEE.

Characteristics of supercontinuum generation under the influence of a weak continuous-wave trigger

Qian Li[1], Feng Li[1], Kenneth K. Y. Wong[2], Alan Pak Tao Lau[1], Kevin K. Tsia[2] and P. K. A. Wai[1,*]

[1]*Photonics Research Centre, Department of Electronic and Information Engineering, The Hong Kong Polytechnic University, Hung Hom, Hong Kong*
[2]*Department of Electrical and Electronic Engineering, The University of Hong Kong, Pokfulam Road, Hong Kong*
[*]*enwai@polyu.edu.hk*

Abstract: We numerically study the impacts of introducing a minute continuous-wave trigger on the properties of picosecond supercontinuum generation; namely the bandwidth, temporal coherence and pulse-to-pulse stability.

Supercontinuum (SC) generation in optical fibers has been the subject of extensive research in the past ten years. Despite the success of SC generation, the stability of SC remains a critical issue in many applications, such as optical frequency metrology, photonic time stretch analog-to-digital conversion, and optical coherence tomography. Although it is well known that SC stability can be greatly improved in SC generation using femtosecond pulses, such ultrashort pulses are sensitive to perturbations and hence are not practical in many applications. SC sources with longer pump pulses (e.g. picosecond or nanosecond) are hence more practical and indeed have mostly been utilized many biophotonics applications. An important nonlinear process in the SC generated with long pulses is modulation instability (MI) which adds sidebands to narrow band input radiation. Since MI growth starts spontaneously from noise, the resulting SC can become incoherent away from the pump wavelength [1]. Prior works have shown the active control of SC can be realized by using a pulse-seed [1] or a THz intensity modulation of the input pulse [2]. Very recently, control of pulse-to-pulse fluctuations in visible supercontinuum is also demonstrated by using a photonic crystal fiber with longitudinally tailored guidance properties [3].

In contrast, we have experimentally demonstrated a simple triggering mechanism to manipulate SC generation by introducing a minute continuous wave (CW) light [4]. Our CW-triggering technique requires only wavelength tuning and does not rely on any phase-locking technique – a much simpler approach to achieve active control of SC. In this paper, we numerically studied how a minute CW trigger could affect the properties of the picosecond SC generation in detail. In particular, we observe that the enhancement in the SC bandwidth in general can be achieved at the expense of temporal coherence, or vice versa. We also find that that depending on the wavelength of the CW-trigger the multiple higher-order, four-wave mixing (FWM) components generated by the CW-trigger can create either a relatively more stochastic or a more deterministic beating effect on the pump pulse, which has a significant effect on the onset of SC in the presence of noise. By simply varying the wavelength of CW-trigger, the rogue solitons emerged in the SC generation can exhibit high-degree of temporal coherence and pulse-to-pulse amplitude stability.

Our simulation is based on the generalized nonlinear Schrödinger equation which includes the full Raman response. Input pulse noise was included in the frequency domain through a (random phase) one photon per mode spectral density on each spectral discretization bin. We simulate a 5.8-ps FWHM chirp-free Gaussian pulse with peak power P_0 = 60 W, and center wavelength at 1554.5 nm propagating in a commercially available 50-m highly nonlinear dispersive fiber (HNL-DSF) with zero dispersion wavelength (ZDW) at 1554.5 nm, nonlinear coefficient γ = 14/W/km, and second order and third order dispersion coefficients at the 1554.5 nm pump wavelength are β_2 = –0.0224 ps^2/km and β_3 = 0.0576 ps^3/km respectively. The CW-trigger power was set to be only 1% of the pump power. By adding a weak CW-trigger at 1716 nm (i.e. at the normalized frequency shift Ω = –400), we observe that the pulse-to-pulse stability can be drastically improved and maintained at a very high level (Fig. 1(c)), compared to the extreme-value and long-tailed statistic shown in the untriggered SC (Fig. 1(a)). The statistical distribution of the CW-triggered SC pulse amplitude has a standard deviation (calculated from 1000 events) as small as 0.01P_0. Furthermore, compared with the case of untriggered SC in which only a narrow band close to the pump center wavelength has relatively good temporal coherence (Fig. 1(b)), the CW-triggered SC shows a better coherence, albeit with the complicated undulation feature. The improvement is especially prominent in the red-shifted Raman soliton (1850 – 2000 nm) range.

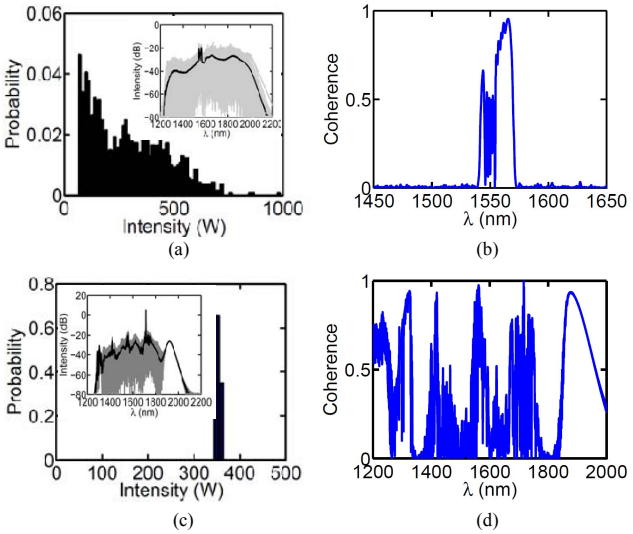

Fig. 1. SC amplitude statistics of (a) the untriggered SC and (c) the triggered SC for Ω=–400. The histograms are plotted for the 1000 events after a long-pass filter (>1850 nm). The insets show the SC spectra from the simulation ensemble (gray) with the calculated average spectrum from the 1000 simulation runs (back). (b) and (d) shows the temporal coherence for the case of (a) and (c), respectively.

978-1-4244-8939-8/11/$26.00 ©2011 IEEE

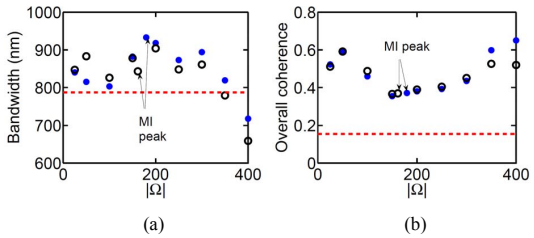

(a) (b)

Fig. 2. (a) Bandwidth of SC spectrum at -50 dB; and (b) overall coherence versus $|\Omega|$, which is the normalized frequency shift of CW trigger with respect to the pump. Dots (open circle) represent the negative (positive) frequency shifts. Dashed line represents the results without CW trigger.

In this particular example, we note that the bandwidth of the CW-triggered SC is actually even narrower than that of the untriggered SC (see the insets of Figs. 1(a) and (c)). This is in contrast to the prior works which generally concluded that the enhancement of SC comes with the temporal coherence improvement. We investigate further by studying the dependence of the SC bandwidth and coherence properties on the CW-trigger wavelengths (Fig. 2). Interestingly, we find that the temporal coherence and the SC bandwidth exhibit the opposite trends as a function of the CW-trigger wavelengths. The coherence bandwidth shrinks to a minimum at $\Omega = -200$ where the SC bandwidth reaches its maximum. It then increases as the CW-trigger wavelength moves further away from the pump whereas the SC bandwidth becomes even narrower than the untriggered case when $\Omega = -400$. This result indeed shows that the effects of the CW-triggering on the SC bandwidth and the temporal coherence are rather subtle.

We also study how the CW-trigger affects the dynamics of the soliton-fission onset – an important clue to understand the temporal stability of the long-pulse SC. It has recently been reported that the initial MI evolution (before the onset of SC) can be interpreted as the Akhmediev Breather (AB) dynamics which develops a modulated temporal profile on the pump pulse [5]. The ABs serve as the precursors for soliton fission by forming the "pre-solitonic" pulses. Fig. 3(a) shows such "pre-solitonic" pulse of the untriggered SC case which exhibits a rather complex and noisy AB feature. In contrast, the "pre-solitonic" pulse in the case of CW-triggered SC (Fig. 3(c) shows a well-defined modulation frequency, which in fact equals to the beating frequency of the CW-trigger and the pump. Simulations show that the higher harmonic frequencies appeared on the pulse is attributed to the beating among other high-order FWM components generated from the CW-trigger.

The AB evolution is now less vulnerable to noise growth and is instead subject to a more deterministic initial condition of soliton fission, i.e. determined by the growing CW-trigger near the MI gain spectrum. Therefore, the Raman soliton emerged from such initial soliton fission process will become more stable. It can be clearly evident from the timing jitters of the Raman solitons in both untriggered SC (Fig. 3(b)) and CW-triggered SC (Fig. 3 (d)). We can see that the pulses are randomly scattered throughout the 40-ps window for the case of untriggered SC (Fig. 3(b)). In contrast, the Raman soliton pulse ensemble is well defined and its timing jitter is as low as ~100 fs for the case of CW-triggered SC (Fig. 3(d)). This explains the high temporal coherence in the red-shifted Raman soliton, as shown in Fig. 1(d).

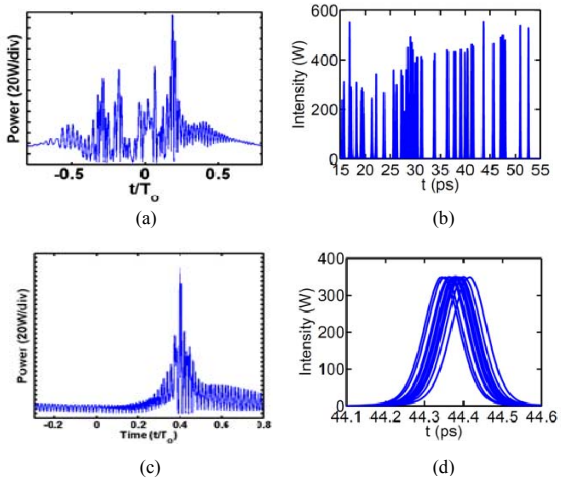

(a) (b) (c) (d)

Fig. 3. (a) and (c) show the "pre-solitonic" temporal pulse shapes (before soliton fission during SC generation) for the untriggered and CW-triggered case ($\Omega = -400$ and $\lambda = 1716$ nm), respectively. (b) and (d) shows the temporal pulses (for clarity, only 20 shots are plotted) after passing the SC spectra through a long-pass filter (>1850 nm) for the untriggered SC, and CW-triggered SC case, respectively.

In conclusion, we performed a detailed numerical study on how the properties of picosecond SC can be influenced by a simple CW triggering scheme. We showed that injecting the weak CW-trigger can alter the SC bandwidth, the overall temporal coherence and the pulse-to-pulse stability, depending on the wavelength of CW-trigger. In particular, the higher-order coherent FWM components generated by the CW-trigger can create a more deterministic beating effect on the pump pulse. This essentially establishes a more well-defined AB condition in the presence of noise – a precursor of the soliton fission and other high-order effects which results in the onset of SC. The presented results would provide a valuable insight on how the initial soliton fission can be initiated in a more controllable manner such that a SC generation with both the high temporal coherence and stability of the SC can be realized.

We acknowledge financial support by grants from the Research Grants Council of the Hong Kong Special Administrative Region, China (Project No. PolyU 5326/09E, HKU 7179/08E, HKU 7183/09E, and HKU 717510E).

References

1. D. R. Solli, C. Ropers, P. Koonath and B. Jalali, Phys. Rev. Lett. **101**, 233902 (2008).
2. G. Gently, J. M. Dudley and B. Eggleton, Appl. Phys. B: Lasers Opt., **94**, 187 (2009).
3. A. Kudlinski, B. Barviau, A. Leray, C. Spriet, L. Héliot and A. Mussot, Opt. Express **18**, 27445 (2010).
4. Kim K. Y. Cheung, Chi Zhang, Yue Zhou, Kenneth K. Y. Wong, and Kevin K. Tsia, Opt. Lett. **36**, 160 (2011).
5. J. M. Dudley, G. Genty, F. Dias, B. Kibler, and N. Akhmediev, Opt. Express 17, 21497-21508 (2009).